SENSOR AND SIMULATION NOTES
NOTE 269

JUNE 1980

THE SINGULARITY EXPANSION METHOD APPLIED TO PERPENDICULAR CROSSED WIRES OVER AN IMPERFECT GROUND PLANE: A SOMMERFELD INTEGRAL FORMULATION

by

Terry T. Crow
Jhi-Chung Kuo
Clayborne D. Taylor

Mississippi State University
Mississippi State, MS 39762

ABSTRACT

The singularity expansion method (SEM) has been applied to determine natural resonances of a horizontal wire and perpendicular crossed wires oriented over an imperfect ground plane. In order to account for the imperfect conductivity of the ground, the Sommerfeld formulation is used and a theoretical-numerical solution obtained. Sample results are presented for both the frequency domain and the SEM solutions.

ACKNOWLEDGMENT: This work was supported through the Air Force Office of Scientific Research, Grant No. AFOSR 78-3667.

SENSOR AND SIMULATION NOTES
NOTE 269

JUNE 1980

THE SINGULARITY EXPANSION METHOD APPLIED TO PERPENDICULAR CROSSED WIRES OVER AN IMPERFECT GROUND PLANE: A SOMMERFELD INTEGRAL FORMULATION

by

Terry T. Crow
Jhi-Chung Kuo
Clayborne D. Taylor

Mississippi State University
Mississippi State, MS 39762

ABSTRACT

The singularity expansion method (SEM) has been applied to determine natural resonances of a horizontal wire and perpendicular crossed wires oriented over an imperfect ground plane. In order to account for the imperfect conductivity of the ground, the Sommerfeld formulation is used and a theoretical-numerical solution obtained. Sample results are presented for both the frequency domain and the SEM solutions.

SEM (singularity expansion method), conductivity, frequency, electromagnetic fields, electromagnetic simulators

ACKNOWLEDGMENT: This work was supported through the Air Force Office of Scientific Research, Grant No. AFOSR 78-3667.

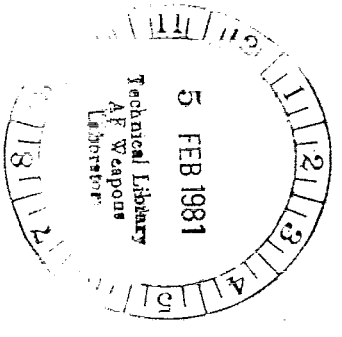

TABLE OF CONTENTS

I. INTRODUCTION

An electromagnetic pulse such as the nuclear EMP or the lightning EMP will induce current and charge densities on aircraft and missile surfaces. These distributions represent the external electromagnetic fields that are in general related linearly to the interior fields (equipment currents and voltages). Acquiring a knowledge of the exterior fields is the first step in determining terminal currents and voltages induced within an illuminated aeronautical system. Transfer functions, either theoretical or experimental, are used to relate the voltage and/or current at a particular location to the most significant point or points of entry for the electromagnetic energy.

A number of simulation facilities have been constructed to test the response of aircraft and missiles to nuclear EMP. Tests can be conducted as an aircraft flies by the simulator but this procedure has its difficulties. Recently a wooden platform has been constructed to simulate in-flight testing while the aircraft sits on the platform; one purpose of such a facility is to decrease ground interactions. In many of the existing facilities the aircraft must rest on a pad of finite conductivity. Thus a theoretical model is needed for the interpretation of the "fly-by" test as well as for the extrapolation of the test data from ground based measurements to predict the inflight mode response.

In contrast to nuclear-EMP testing lightning-EMP testing has not evolved to the level of sophistication of nuclear EMP testing.

Probably this is a result of the lightning pulse not being well defined and the accompaning nonlinear environment not being well understood. However lightning-EMP testing requires many of the same considerations as nuclear-EMP, simulating the appropriate electromagnetic environment and quantifying the effects of the physical limitations of the simulator configuration.

In order to gain insight into the response of an aircraft or missile to an electromagnetic pulse, a wire model is used for both convenience and accuracy [1]. When an aircraft/missile (or the wire model) is located near an imperfect ground plane as in the usual test configuration, the induced surface currents are affected by two principle processes. First, the scatterer is exposed to the direct radiation and the ground reflected radiation. Second, the induced surface currents interact with the ground plane. The first process is well understood for both perfect and imperfect ground planes, and is straight forward to analyze [2]. However the second process being much more complicated is very difficult to analyze, particularly when the ground is an imperfect conductor [3].

A general formulation based on the singularity expansion method is developed for horizontal wire scatterers oriented over an imperfect ground plane. In order to account for the imperfect conductivity the exact Sommerfeld formulation is used [4]. Accordingly a system of integral equations are derived and solved utilizing a numerical solution technique. Natural frequencies for a single horizontal wire and for a horizontal wire cross are obtained.

Because of the complexity of the Sommerfeld integrals as they

appeared in the kernel of the integral equations the computer CPU time would be prohibitive for a parametric study. Therefore sufficient data is presented only for fiducial purposes. Frequency domain results for plane wave excitation are presented along with natural frequencies.

II. FORMULATION

Frequency Domain Considerations

For an arbitrary configuration of horizontal wires oriented over an imperfect ground plane the individual wire currents induced by an incident electromagnetic field are obtained by solving a system of linear integral equations [5].

$$\sum_{i=1}^{N} \int_{L_i} I_i(\ell'_i) G(\ell_j, \ell'_i) d\ell'_i = j4\pi\omega\epsilon_o (E_{tj}^{inc} + E_{tj}^{ref}) \qquad (1)$$

where E_{tj}^{inc} and E_{tj}^{ref} are the components of the incident and ground reflected electric fields along the jth wire of a system of N wires, $I_i(\ell'_i)$ is the current on the ith wire at position ℓ'_i,

$$G(\ell_j, \ell'_i) = \cos(\alpha_j - \alpha_i)\{(\frac{\partial^2}{\partial x^2} - \gamma_o^2)(g_o - g_1 + g_{SH} + g_v) + \gamma_o^2 g_v\}$$

$$+ \sin(\alpha_j - \alpha_i) \frac{\partial^2}{\partial y \partial x} (g_o - g_1 + g_{SH} + g_v) \qquad (2)$$

$$g_o = \frac{e^{-\gamma_o R_o}}{R_o} \qquad (3)$$

$$g_1 = \frac{e^{-\gamma_o R_1}}{R_1} \qquad (4)$$

$$g_{SH} = 2 \int_0^\infty \frac{e^{-u_o(z+z_o)}}{u_o + u_1} J_o(\lambda\rho)\lambda d\lambda \qquad (5)$$

$$g_v = -2 \int_0^\infty \frac{(u_o - u_1) e^{-u_o(z + z_o)}}{\gamma_o^2 u_1 + \gamma_1^2 u_o} J_o(\lambda\rho)\lambda d\lambda \tag{6}$$

$$R_o = \sqrt{(z-z_o)^2 + p^2} \tag{7}$$

$$R_1 = \sqrt{(z+z_o)^2 + \rho^2} \tag{8}$$

$$\rho = \sqrt{x^2 + y^2} \tag{9}$$

$$u_o = \sqrt{\lambda^2 + \gamma^2} \tag{10}$$

$$u_1 = \sqrt{\lambda^2 + \gamma_1^2} \tag{11}$$

$$\gamma_o = j\omega\sqrt{\mu_o \varepsilon_o} = jk_o \tag{12}$$

$$\gamma_1 = \sqrt{j\omega\mu_1(\sigma_1 + \omega\varepsilon_1)} \tag{13}$$

$$x = (x_j - x'_i)\cos\alpha_i + (y_j - y'_i)\sin\alpha_i \tag{14}$$

$$y = -(x_j - x'_i)\sin\alpha_i + (y_j - y'_i)\cos\alpha_i \tag{15}$$

$$z = z_o \tag{16}$$

Here (x'_i, y'_i, z_o), the coordinates of ℓ'_i along the ith wire; (x_j, y_j, z_o), the coordinates of points ℓ_j along the jth wire; and the angles α_i and α_j are illustrated in Figure 1.

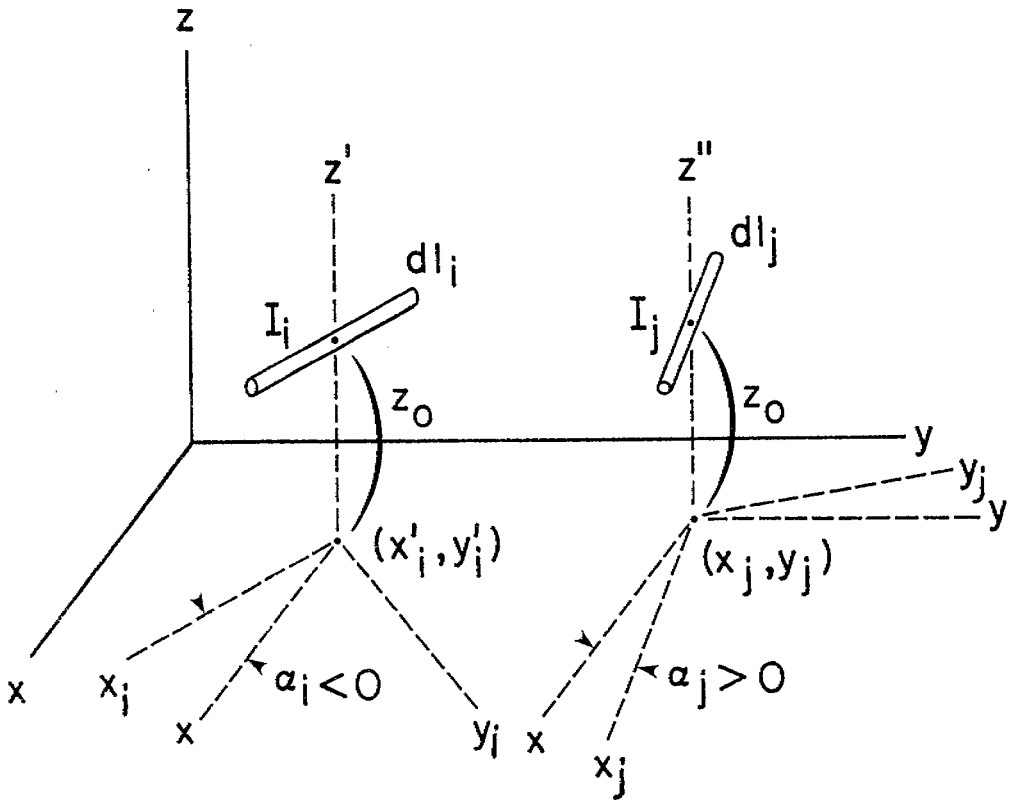

Figure 1: Two horizontal wire segments above an imperfect ground, $z \leq 0$.

When the horizontal wires are joined additional considerations must be made. First the wires must satisfy Kirchhoff's current law, the sum of the wire currents must equal zero at the junction. Second the charge per unit length on the wires are required to satisfy the Wu-King [6] junction condition, i.e. for an n-wire junction

$$q_1\psi_1 = q_2\psi_2 = q_3\psi_3 = \text{---} = q_n\psi_n \tag{17}$$

where q_i is the charge per unit length given by

$$q_i = -\frac{1}{j\omega}\frac{d}{d\ell_i} I_i(\ell_i)\Big|_{\text{junction pt.}} \tag{18}$$

and

$$\psi_i = 2\left[\ell n\left(\frac{2}{k_o a_i}\right) - 0.5772\right] \tag{19}$$

In addition to the junction conditions the wire currents are required to vanish at the open ends.

Due to the complexity of the system of integral equations to be solved a numerical solution technique is employed, in particular, the method of moments. This procedure involves dividing the wire structure into electrically short segments. On each segment, the wire current is approximated by some convenient function, here a sinusoidal current expansion is used. Therefore the current on the nth segment of the jth wire with end currents $I_j(\ell_j,n)$ and $I_j(\ell_j,n+1)$ is represented by

$$I_j(\ell_j) =$$

$$\frac{I_j(\ell_{j,n+1}) \sin [k_o(\ell_j - \ell_{j,n})] + I_j(\ell_{j,n}) \sin [k_o(\ell_{j,n+1} - \ell_j)]}{\sin[k_o(\ell_{j,n+1} - \ell_{j,n})]} \tag{20}$$

Upon introducing the segmental current representation into the system of integral equations, a system of linear equations for the segment end currents can be obtained by enforcing the resulting equations at a discrete set of points, namely, the end points of the wire segments.

The resulting system of linear equations is of the form

$$\sum_{n=1}^{N} S_{mn} I_n = E_m \tag{21}$$

where $N=N_1+N_2+N_3+$ --- is the total number of unknown currents after requiring the currents at the open ends to be zero. The integral equation is enforced at the ends of all wire segments excluding open wire ends and junction points, which yields $N-N_w$ equations where N_w is the total number of wires intersecting. Applying the Wu-King junction condition yields $N_w - N_J$ equations where N_J is the total number of junctions. Applying the Kirchhoff current law at the junctions yields an additional N_J equations. Hence the total number of equations is equal to N, the total number of unknown currents.

Computation of the system matrix elements S_{mn} can be simplified by mathematical manipulation and integration by parts. However the Sommerfeld terms accouting for the imperfect ground require a double numerical integration, one integral over the wire segment

and the other integral over an infinite range. These integrals occur in the expressions for g_{SH} and g_v, see (5) and (6). To perform the evaluation a deformed contour similar to the one suggested by Miller et al [7] is chosen. The deformation of the contour is permissable since all the branch points and poles of the integrand lie in the second and forth quadrants of the complex λ plane. Accordingly

$$g_{SH} = 2j \int_0^{\lambda_I} \frac{\exp[-j\sqrt{\lambda^2-\gamma_o^2}\ (z+z_o)]}{\sqrt{\lambda^2-\gamma_o^2}+\sqrt{\lambda^2-\gamma_1^2}}\ I_o(\lambda\rho)\lambda d\lambda$$

$$+\ 2 \int_0^{\infty} \frac{\exp[-\sqrt{\beta^2-\gamma_o^2}\ (z+z_o)]}{\sqrt{\beta^2-\gamma_o^2}+\sqrt{\beta^2-\gamma_1^2}}\ J_o(\beta\rho)\beta d\lambda \qquad (22)$$

$$g_v = -2j \int_0^{\lambda_I} \frac{\sqrt{\lambda^2-\gamma_o^2}\left(\sqrt{\lambda^2-\gamma_o^2}-\sqrt{\lambda^2-\gamma_1^2}\right)\exp[-j\sqrt{\lambda^2-\gamma_o^2}\ (z+z_o)]}{\gamma_o^2\sqrt{\lambda^2-\gamma_1^2}+\gamma_1^2\sqrt{\lambda^2-\gamma_o^2}}$$

$$\times\ I_o(\lambda\rho)\lambda d\lambda$$

$$+2 \int_0^{\infty} \frac{\sqrt{\beta^2+\gamma_o^2}\left(\sqrt{\beta^2+\gamma_o^2}-\sqrt{\beta^2+\gamma_1^2}\right)\exp[-\sqrt{\beta^2+\gamma_o^2}\ (z+z_o)]}{\gamma_o^2\sqrt{\beta^2+\gamma_1^2}+\gamma_1^2\sqrt{\beta^2+\gamma_o^2}}$$

$$\times\ J_o(\beta\rho)\beta d\lambda \qquad (23)$$

where $\beta = \lambda + j\lambda_I$ and I_o is the modified Bessel function of the first kind. The choice of λ_I, a real constant, as the limit of the first integrals in (22) and (23) is made to render the integrands of the second integrals sufficiently smooth for rapid convergence when a Gaussian-Laguerre interpolatory quadrature

formula is used. For real frequencies $\lambda_I = 5k_o/2\pi$ provides good results. Some experimentation is required to choose an appropriate value for λ_I when complex frequencies are considered. The first integrals in (22) and (23) are evaluated by using the Gaussian interpolatory quadrature.

Both the Gaussian and Gaussian-Laguerre quadrature formulas are derived by using convenient interpolating polynomials. Theoretically, the more roots of the polynomials (increasing the order) the more accurate the results will be. However this occurs at the expense of computer CPU time. For the data that will be presented subsequently, the number of roots of the Gaussian quadrature is denoted NIG and the number of roots for the Gaussian-Laguerre quadrature is NIL. Both NIG and NIL are varied to achieve the desired accuracy within the limitations of available CPU time.

Singularity Expansion Method

In order to employ the singularity expansion method (SEM) the foregoing frequency domain formulation is extended into the complex s-plane, where $s = j\omega$. Basically the SEM solution technique provides a solution for the induced current in terms of a simple pole expansion in the frequency domain and corresponding damped sinusoids in the time domain. To construct the solutions one must obtain the natural frequencies (poles), natural modes and coupling coefficients [8]. Only the natural frequencies are expected to sensitive to the properties of an imperfect ground plane. Hence this report will concentrate on obtaining data for the natural frequencies.

The natural frequencies are the simple poles of the solutions for the surface current and charge in the complex s-domain. In order to obtain the natural frequencies the system of equations in (21) are used. By observing that the singularities of the current are those complex frequencies for which the system matrix is singular, i.e. $\det[S_{mn}] = 0$, the natural frequencies are obtained by searching for the roots of the determinant of the system matrix. For the data reported here the roots were obtained via a Muller iteration scheme [9].

III. FREQUENCY DOMAIN RESULTS

In order to verify the numerical procedures and algorithms frequency domain, domain data is obtained for two simple wire configurations, a single horizontal wire and a horizontal wire cross. Both configurations have been studied extensively by other authors for both free space conditions and perfect ground plane conditions [10,11].

The single horizontal wire oriented over an imperfect ground is illustrated in Figure 2. For plane wave incidence normal to the ground and with the electric field directed parallel to the cylinder, typical induced axial currents are exhibited in Figure 3 for resonant conditions (for comparison see Table 5). Corresponding results for a perfect ground would show significant variation of the current magnitude with height above the ground. From the analysis of Taylor et al. [12] one obtains for the current at the center of the horizontal wire

$$I = j \frac{UE^{inc}}{kZ_c} \left[\frac{\cos(k\ell/2)-1}{\cos(k\ell/2)} \right] \tag{24}$$

where

$$U = \frac{2\eta_g}{\eta_g+\eta_o} + jk_o \ell n \frac{2\eta_o}{\eta_g+\eta_o} \tag{25}$$

$$Z_c = Z_{co} \left\{ 1 + \frac{\ell n \frac{1+\gamma h}{\gamma h}}{\ell n \frac{2h}{a}} \right\}^{\frac{1}{2}} \tag{26}$$

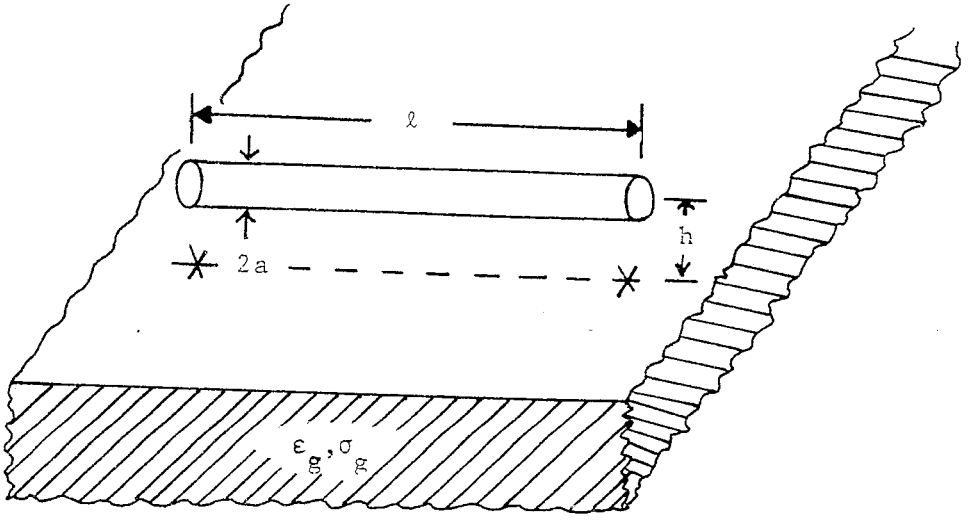

Figure 2: Single horizontal cylinder oriented over an imperfect ground plane.

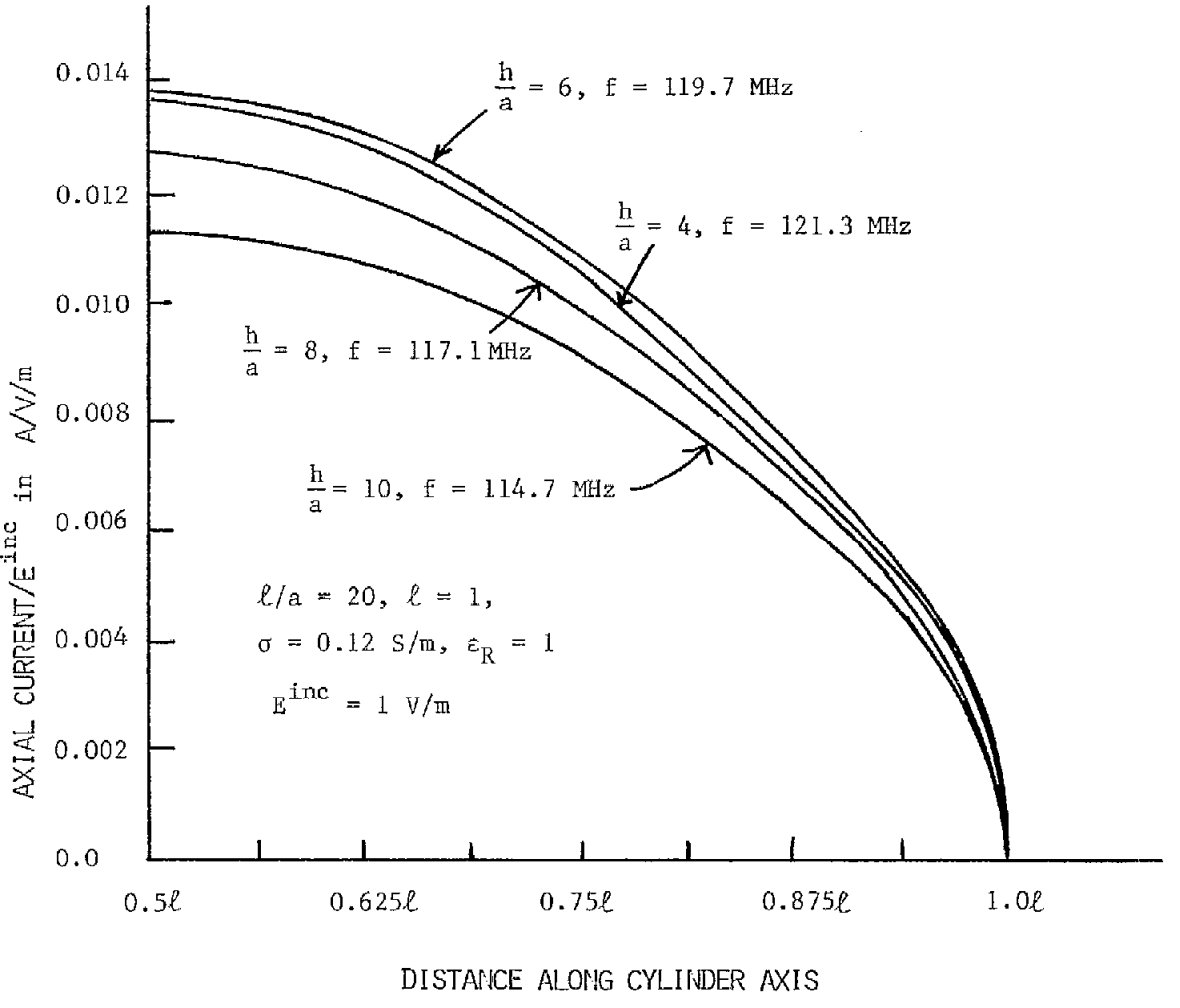

Figure 3: Current distribution along a horizontal cylinder over an imperfect ground and illuminated by a plane wave propagating normal to the ground with the electric field directed parallel to the cylinder.

$$k = k_o \left\{ 1 + \frac{\ell n \frac{1+\gamma h}{\gamma h}}{\ell n \frac{2h}{a}} \right\}^{\frac{1}{2}} \tag{27}$$

$$Z_{co} = \frac{\eta_o}{2\pi} \ell n \frac{2h}{a} \tag{28}$$

$$\eta_o \simeq 120\,\pi$$

$$\eta_g = \sqrt{\frac{\mu_o}{\varepsilon_g - j\frac{\sigma_g}{\omega}}}$$

$$\gamma = [j\omega\mu(\sigma_g + j\,\omega\varepsilon_g])^{\frac{1}{2}}$$

For the parameters presented in Figure 3, (24) yields

$$\frac{|I|}{E^{inc}} \simeq 0.0108 \angle 38.4^{\circ} \quad \text{A/V/m}$$

when $h/a = 4$ and $f = 119.7$ MHz. The agreement between the foregoing result and the numerically obtained value in Figure 3 is satisfactory since (24) was derived using transmission line theory that requires $(k_o h)^2 << 1$ whereas the sample calculation considered $k_o h = 0.501$.

A second configuration is also considered. It is a horizontal wire cross oriented over an imperfect ground as shown in Figure 4. With the structure illuminated from above and the electric field directed parallel to the ℓ_1 and ℓ_1' elements, the current distributions are computed and displayed in Figure 5.

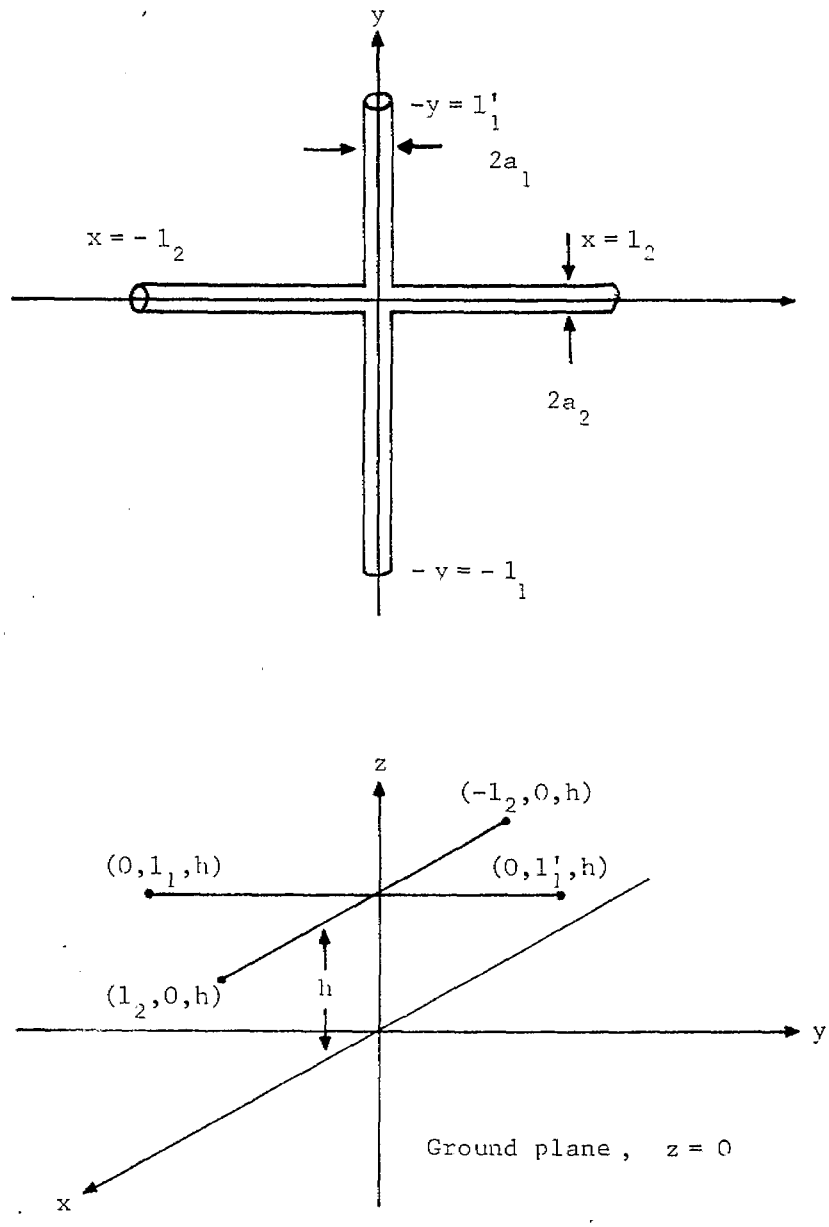

Figure 4. The orthogonal crossed wire configuration over a ground plane.

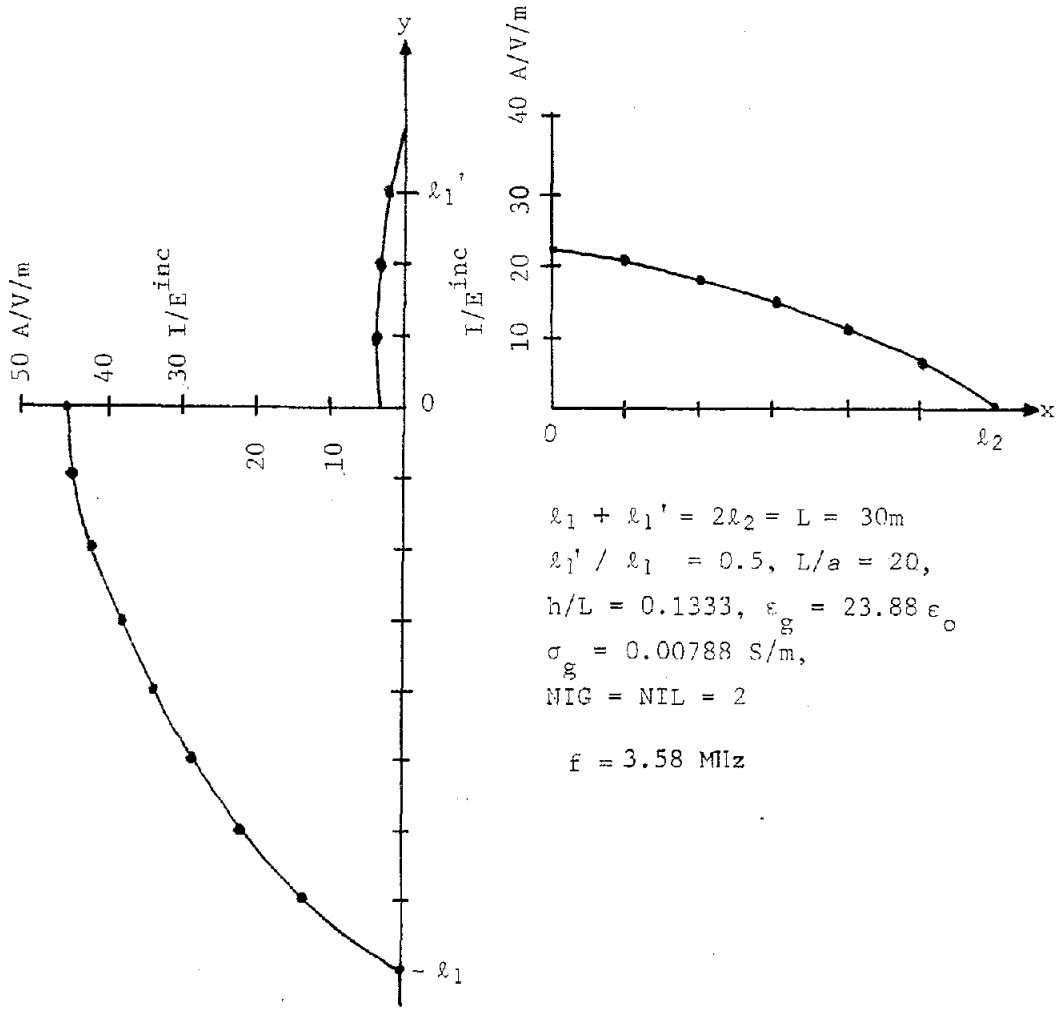

Figure 5: Current distribution induced on perpendicular crossed cylinders oriented horizontally over an imperfect ground plane for plane wave illumination propagating normal to the ground with the electric field parallel to the y-axis.

IV. SINGULARITY EXPANSION METHOD RESULTS

In order to have confidence in the numerically obtained results the dependence of the results upon the various numerical solution parameters is investigated. Considering the single cylinder, Table 1 illustrates typical dependence on the parameters used to evaluate the Sommerfeld integrals (22) and (23). At the lower conductivity substantial variation in the first natural frequency is exhibited. Also the natural frequencies depend upon the number of current segments used. This dependence is exhibited in Table 2. Generally when the length of a current segment is greater than a/z and less than 2a, good results are obtained. Finally the numerically obtained results are compared with the results of independent (but less rigorous) formulations. These data are shown in Table 3.

Obtaining the natural frequencies for various ground conductivities becomes increasingly more difficult as the conductivity is decreased. In Figure 6 the natural frequencies of a cylinder are displayed in the complex s-plane with conductivity of the ground as a parameter. For high conductivities the natural frequencies approach the value obtained for a perfect ground [10]. But for low conductivities numerical difficulties begin to occur for $\sigma_g \lesssim 0.1$ S/m, which prevented convergence to the free space result. The dotted line is expected to give the true variation.

TABLE 1: First Natural Frequency of a Cylinder over an Imperfect Ground for Various Numerical Parameters

($\ell/a=20.$, $h/a=4$, $\ell=1m$, $\varepsilon_R=1$)

σ	NIG	NIL	γ_I	$s_1\ell/c$
1.2S/m	4	4	$5k_o/2\pi$	$-0.1598 + j\,2.551$
	6	6	$5k_o/2\pi$	$-0.1598 + j\,2.551$
	6	15	$5k_o/2\pi$	$-0.1566 + j\,2.565$
0.06S/m	6	15	$7k_o/2\pi$	$-0.460 + j\,2.584$
	6	15	$9k_o/2\pi$	$-0.442 + j\,2.650$
	6	15	$11k_o/2\pi$	$-0.423 + j\,2.719$

TABLE 2: First Natural Frequency of a Cylinder over an Imperfect Ground Versus the Number of Current Segments

($\ell/a=200$, $h/a=40$, NIL = NIG = 2, $\ell=1m$, $\sigma = 1.2 \times 10^8$ S/m, $\varepsilon_R=1$)

N	$s_1\ell/c$
10	$-0.0293 + j\,3.061$
16	$-0.0392 + j\,3.018$
25	$-0.0481 + j\,2.980$
40	$-0.0549 + j\,2.925$
50	$-0.0570 + j\,2.906$
80	$-0.0593 + j\,2.878$

TABLE 3: First Natural Frequency of a Cylinder over an Imperfect Ground as Obtained by Different Analyses.

($\ell/a=20$, $h/a=4$, $\ell=1m$, $\sigma=120\ S/m$, $\varepsilon_R=1$)

ANALYSIS	$s_1\ell/c$
Sommerfeld-Integral Formulation	$-0.0915 + j\ 2.599$
Riggs and Shumpert [13]	$-0.0875 + j\ 2.526$
Reflection Coefficient Formulation [14]	$-0.1246 + j\ 2.562$

TABLE 4: First Natural Frequency of a Cylinder over an Imperfect Ground versus Dielectric Constant.

($\ell/a=20.$, $h/a=4$, $\ell=1.0m$, $\sigma=0.12\ S/m$)

ε_R	$s_1\ell/c$
1	$-0.3320 + j\ 2.5182$
10	$-0.3135 + j\ 2.5856$
20	$-0.2741 + j\ 2.6140$
25	$-0.2594 + j\ 2.6189$
35	$-0.2379 + j\ 2.6232$

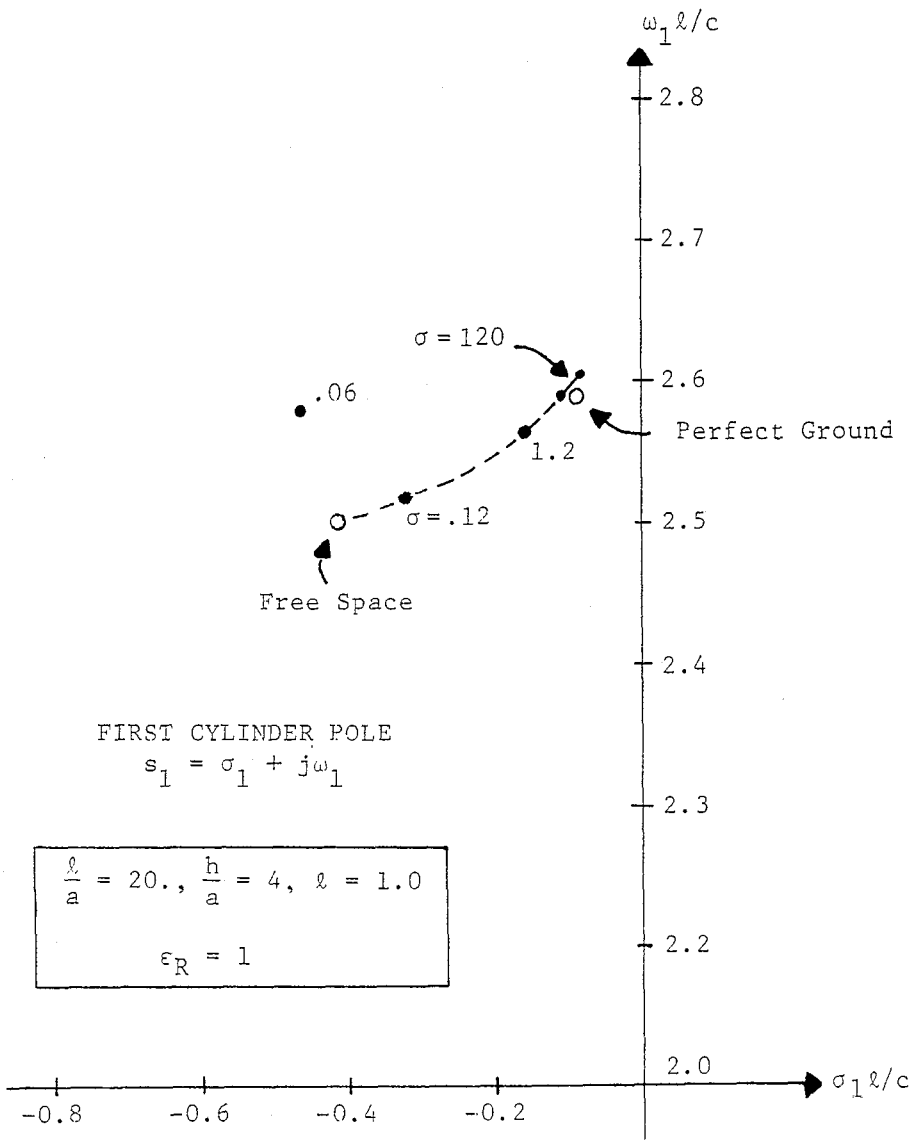

Figure 6: First Natural Frequency of a horizontal cylinder over an imperfect ground plane versus ground conductivity

Note that when numerical difficulties occur the natural frequency is close to the free space value.

The dependence of the natural frequencies of a horizontal cylinder upon the permittivity of the ground and the height above the ground is exhibited in Tables 4 and 5. These data are not intended to be sufficient to provide the complete parametric behavior. They are presented to be a basis of comparison for a more efficient (i.e. less expensive) algorithm developed by using an approximate solution technique.

TABLE 5: First Natural Frequency of a Cylinder over an Imperfect Ground Versus Height.
($\ell/a=20.$, $\ell=1.0$m, $\sigma=0.12$S/m, $\varepsilon_R=1$)

h/a	$s_1\ell/c$
4	-0.3320 + j 2.5182
6	-0.2940 + j 2.4899
8	-0.3133 + j 2.4324
10	-0.3511 + j 2.3768
∞	-0.4242 + j 2.503

TABLE 6: Natural Frequencies of Horizontal Crossed Wires over an Imperfect Ground ($\ell_1+\ell_1'=L=2\ell_2$, $L/a=20$, $\ell_1'/\ell_1=0.5$, $h/L=0.2$, $L=1$m, $\sigma=0.1$S/m, $\varepsilon_g=20\varepsilon_o$)

Mode	sL/c		
	Free Space	Perfect Ground	Imperfect Ground
sy,1,1	-0.2923 + j 2.319	-0.0513 + j 2.361	-0.0965 + j 2.222
sy,1,2	-0.3426 + j 3.726	-0.1021 + j 3.769	-0.0927 + j 3.715
sy,2,2	-0.6786 + j 6.066	-0.3909 + j 5.741	-0.44 + j 5.781
sy,3,1	-1.0166 + j 8.139	-0.6691 + j 7.581	-0.69 + j 7.59
as,1	-0.4242 + j 2.503	-0.0898 + j 2.592	-0.2621 + j 2.620

V. CONCLUSION

By extending the Sommerfeld formulation treating infinitesimal dipoles over an imperfect ground plane, a formulation is developed for treating horizontal wire configurations in proximity to an imperfect ground. Numerical results are obtained for a single wire and perpendicularly crossed wires.

Structure resonances are obtained by utilizing the singularity expansion method. Sample results are presented and comparisons are made with the results of other more approximate formulations. Because of the inordinant amount of CPU time required parameter studies are not presented. However sufficient data are provided to verify more efficient algorithms that may be developed.

VI. REFERENCES

1. C. D. Taylor, "External Interaction of the Nuclear EMP with Aircraft and Missiles," IEEE Trans. on Ant. and Prop., Vol. AP-26, pp. 64-76, January 1978.

2. J. A. Stratton, Electromagnetic Theory, McGraw-Hill, New York, 1941, Sec. 9.9.

3. T. K. Sarkar and B. J. Strait, "Analysis of Arbitrarily Oriented Thin Wire Antenna Arrays over Imperfectly Conducting Ground Planes," Syracuse University Technical Report TR-75-15, December 1975.

4. A Sommerfeld, Partial Differential Equations in Physics, Academic Press, New York, 1964.

5. C. D. Taylor, K. T. Chen, and T. T. Crow, "A Study of Horizontal Wire Scatterers over an Imperfect Ground Plane, Final Report, Vol. III," prepared for Air Force Office of Scientific Research Grant No. AFOSR-77-3342, September 1978.

6. T. T. Wu and R. W. P. King, "The Tapered Antenna and its Application to the Juntion Problem for Thin Wires," IEEE Trans. on Ant. and Prop., Vol. AP-24, pp. 42-46, January 1976. Also see Interaction Note 269, AFWL, January 1976.

7. E. K. Miller, A. J. Poggio, G. J. Burke and E. S. Selden, "Analysis of Wire Antennas in the Presence of a Conducting Half-space: Part II. The Horizontal Antenna in Free Space,: Canadian J. of Phys., Vol. 50, pp. 2614-2626, 1972.

8. C. E. Baum, "The Singularity Expansion Method," Topics in Applied Physics, Vol. 10, 1976 (Editor, L. B. Felson).

9. T. T. Crow, B. D. Graves, and C. D. Taylor, "The Singularity Expansion Method as Applied to Perpendicular Crossed Wires," IEEE Trans. on Ant. and Prop., Vol. AP-23, pp. 540-546, July 1975. Also see Interaction Note 161, AFWL, Oct. 1973.

10. T. T. Crow, C. D. Taylor, and M. Kumbale, "The Singularity Expansion Method Applied to Perpendicularly Crossed Wires Over a Perfectly Conducting Ground Plane," IEEE Trans. on Ant. and Prop., Vol. AP-27, pp. 248-252, March 1979. Also see Sensor and Simulation Note 258, AFWL, June, 1979.

11. T. H. Shumpert and D. J. Galloway, "Finite Length Cylindrical Scatterer Near Perfectly Conducting Ground--a Transmission Line Mode Approximation," IEEE Trans. on Ant. and Prop., Vol. AP-26, pp. 145-151, January 1978. Also see Sensor and Simulation Note 226, AFWL, Aug., 1976.

12. C. D. Taylor, V. J. Naik, and T. T. Crow, "A Study of the EMP Interaction with Aircraft over an Imperfect Ground," Interaction Note 362, Air Force Weapons Laboratory, Kirtland AFB, N.M., May 1979.

13. L. S. Riggs and T. H. Shumpert, "Trajectories of the Singularities of a Thin-wire Scatterer Parallel to Lossy Ground," IEEE Trans. on Ant. and Prop., Vol. AP-27, pp.864-869, November 1979.

14. T. T. Crow, Y. Hsu and C. D. Taylor, "The Natural Resonances of Perpendicular Crossed Wires Parallel to an Imperfect Ground Using SEM and Fresnel Reflection Coefficients," Sensor and Simulation Note 268, Air Force Weapons Laboratory, Kirtland AFB, N.M., June 1980.